Pertanika J. Sci. & Technol. 25 (4): 1357 - 1368 (2017)

SCIENCE & TECHNOLOGY

Journal homepage: http://www.pertanika.upm.edu.my/

ISDA based Precise Orbit Determination Technique for Medium Earth Orbit Satellites

Mishra, S.[1,3], Singh, G.[2], Singh, M.[1,3] and Gaba, G. S.[1,3]*

[1]*Discipline of Electronics and Communication Engineering, Lovely Professional University, Jalandhar, India*
[2]*Dr. A.P.J. Abdul Kalam Technical University, Lucknow, India*
[3]*Lovely Professional University, Jalandhar, India*

ABSTRACT

The satellite orbit determination approach involves a set of techniques which measure the satellite motion in terms of its velocity and position. In this paper, we have elaborated the method of determining an accurate ephemeris for an orbiting satellite which involves estimating the position and velocity of the satellite from a sequence of observations. To observe perturbations in the orbit due to different types of gravitational and non-gravitational effect, we have applied the prediction algorithm and analysed the changes in the Kepler's elements. Dynamic and static errors are the limiting factors for estimation techniques, such as the geo-potential model errors and atmospheric drag model errors, depending on the dynamic environment of the satellite. The proposed prediction model can help to prevent the loss of control over the satellite due to orbital variations.

Keywords: Atmospheric drag, Estimation techniques, Gauss theory, Inter Satellite Distance, Kalman filtering, Kepler elements, Non-gravitational forces

INTRODUCTION

The main requirement of the orbit determination is to find out the position of the object and its motion in various directions, in order to identify the actual position and drift. The inter satellite communication is where neighbouring satellites communicate with each other for various applications (Yang, Yue, & Dempster, 2016). For the Global Navigation Satellite system, consider the MEO constellation which includes 24 satellites and 3 orbital distributions with

ARTICLE INFO

Article history:
Received: 05 June 2017
Accepted: 23 September 2017

E-mail addresses:
mshivam383@gmail.com (Mishra, S.),
munish.17486@lpu.co.in (Singh, G.),
nitgagan@gmail.com (Singh, M.),
er.gurjotgaba@gmail.com (Gaba, G. S.)
*Corresponding Author

ISSN: 0128-7680

55-degree inclination angle (Yu, Yang, & Ding, 2013). The orbit determination technique is based on estimation of drift, which in turn is used to predict the future orbit (Barrio & Serrano, 2008; Hobbs & Bohn, 2006; Kuznetsov, 2016). Various orbit determination schemes have been evolved in the past era out of which few emerging techniques use the principle of Kalman filtering (Pardal, Kuga, & de Moraes, 2009), Extended Kalman Filtering, and Gauss Method. Yang et al. (2016) describes three classes for absolute Global Navigation: purely kinematic, accurate dynamic and reduced dynamic scheme. The reduced dynamic orbit determination is achieved by high prediction ability of the earth orbiters which is also used in conjunction with GPS to provide a more accurate solution than Global Navigation Systems (Ali & Montenegro, 2014).

The requirement of the orbit determination is because of induced satellite drift as a result of gravitational and non-gravitational effects. The gravitational forces that act on satellite are centripetal and centrifugal force, while the non-gravitational effects are the atmospheric drag (Kandula, Kumar, & Bhasker, 2016; Moe & Moe, 2011), solar radiation pressure (Al-Bermani, 2010), third-body perturbations, Earth tidal effects (Pardal et al., 2009). For the Global Navigation satellite orbit determination, there are generally two coordinate systems: the earth centred earth fixed and earth centred inertial system provide the coordinates of the satellite as well as other objects established in the space. For orbit determination, the orbital parameters should be first calculated (Yi et al., 2016). The satellite orbital Keplerian motion is mainly defined by the six orbital parameters which are listed in Table 1. The Global Navigation Satellite System is established in the MEO at the mean distance of 26,560km from the middle of the earth (Zaminpardaz, Teunissen, & Nadarajah, 2017). With a mean earth radius of 6360km, the height of the MEO (Medium Earth Orbit) is about 20,200km (El-naggar, 2012).

Table 1
Six Orbital Parameters

Keplerian Parameter	Notation
a	Semi-major Axis
e	Eccentricity
I	Inclination Angle
ω	Argument of Perigee
Ω	Right Ascension of Ascending Node
M	Mean Anomaly

Adapted from National Aeronautics and Space Administration. Copyright 2017 by National Aeronautics and Space Administration. In the public domain.

The rest of the paper is organised as follows: Section II defines the orbit perturbations due to atmospheric effects. Methodology is discussed in section 3, followed by a discussion of results in section 4. Section 5 concludes the paper.

Orbital Perturbations due to Atmospheric Effect

Centripetal and centrifugal force. The two gravitational forces try to pull the satellite inwards and outwards. However, their effect cancels out and helps the satellite to stabilise its orbit in space. Due to the elliptical orbit, the strength of gravitational forces is different at the different sectors of orbital path, which makes it important to go for dynamic orbit determination. The gravitational forces are centripetal which pull the object inwards due to gravity and the centrifugal forces pull outwards to control the orientation of the satellite orbit. These forces are represented in equation 1, 2 and 3.

$$F_{centripetal} = -\frac{G\,Me\,m}{r^2} \tag{1}$$

$$F_{centrifugal} = \frac{m\,v^2}{r} \tag{2}$$

$$v = \sqrt{G\,Me/r} \tag{3}$$

Atmospheric drag. Atmospheric drag causes drift in the satellite motion and path due to variations in atmospheric density, ballistic parameter, aperture area and mass of the satellite. The atmospheric drag force is the reason behind the altitude fluctuations of the satellite w.r.t. time as shown in Figure 1 and represented in Equation 4.

$$F_{drag} = -\frac{1}{2}\frac{\rho C_d\,A}{m}v^2 \tag{4}$$

Where,

ρ is atmospheric density
m is mass of satellite
A is cross sectional area
v is velocity of satellite
C_d is drag coefficient

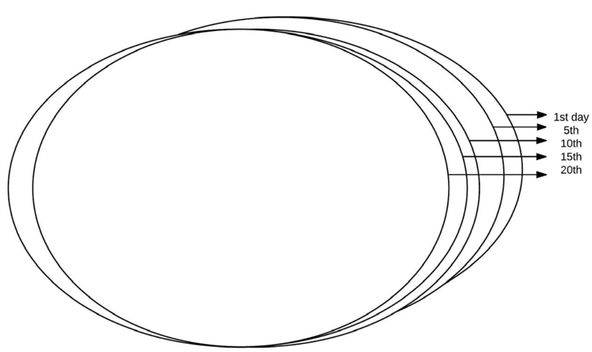

Figure 1. Orbit Deviation due to Atmospheric Effect. Adapted From "Trajectory Control During an Aeroassisted Maneuver Between Coplanar Circular Orbits," by W. G. D. Santos, E. M., Rocco, and V. Carrara, 2014, *Journal of Aerospace Technology and Management, 6*(2), p. 160. Copyright 2014 by Journal of Aerospace Technology and Management

METHODOLOGY

Step 1

In the space segment, the satellite trajectory has different coordinates which is followed continuously by the satellite, thus, forming an orbit. The global navigation satellite systems are operated at Medium Earth Orbit. To find out the satellite Cartesian coordinates, we need to apply the formula provided in equations 5, 6, 7, and 8 to get the initial coordinates of the satellite, followed by transformation of cylindrical coordinates system through transformation algorithm. To find out the distance between the two satellites, pseudo range formula is applied.

$$X_{initial} = r[\cos(\omega + \theta)\cos\Omega - \cos i \sin(\omega + \theta)\sin\Omega \tag{5}$$

$$Y_{initial} = r[\cos(\omega + \theta)\sin\Omega - \cos i \sin(\omega + \theta)\cos\Omega \tag{6}$$

$$Z_{initial} = r[\sin(\omega + \theta)\sin i \tag{7}$$

$$r = \frac{a(1-e^2)}{1+e\cos\theta} \tag{8}$$

After finding the initial coordinates of both the satellites, we need to find out the inter satellite distance through equation 9 to analyse the effect of perturbations on neighbouring satellites.

$$D = \sqrt{(X_{initial} - X_1)^2 + (Y_{initial} - Y_1)^2 + (Z_{initial} + Z_1)^2} \tag{9}$$

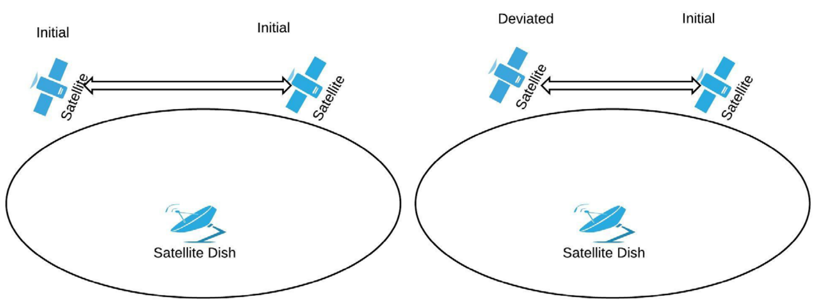

Figure 2. IniFtiiagl uarned 2D. eIvniiatitaeld aInndte rD Seavtiealltietde DInitsetar nScaet edluleit eto D piesrttaunrbcaet idounes to perturbations

The effect of atmospheric forces on cylindrical coordinates of Satellite orbit can be well understood through equations 10, 11, 12.

$$F_r = -\frac{1}{2}\frac{C_d}{m}\frac{A\rho}{}\frac{\mu}{a}e^{\alpha\, cosE}\frac{(1+e\cos E)^{1/2}}{(1-e\cos E)^{3/2}}e\sin E \tag{10}$$

$$F_{\theta =} -\frac{1}{2}\frac{C_d}{m}\frac{A\rho}{}\frac{\mu}{a}e^{\alpha\, cosE}\frac{(1+e\cos E)^{1/2}}{(1-e\cos E)^{3/2}}(1-e^2)^{1/2} \tag{11}$$

$$F_{z=} - \frac{1}{2}\frac{C_d}{m}\frac{A\rho}{}\frac{\mu}{a}e \tag{12}$$

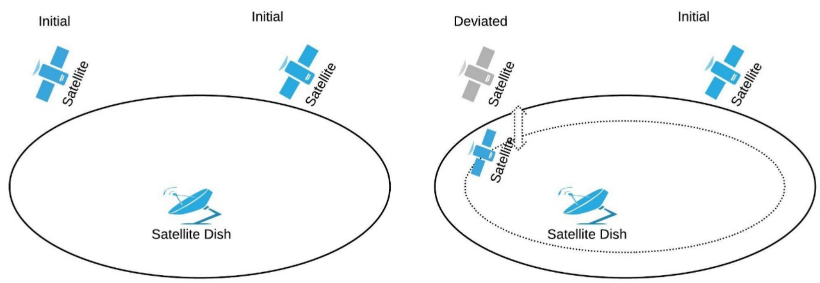

Figure 3. Initial and Deviated Orbit of Satellite due to Perturbations

Step 2

The atmospheric drag is a major reason behind the variations in the orbital parameters. The orbital determination parameter such as semi-major axis and eccentricity are more affected due to the atmospheric drag in addition to reduced velocity of the global navigation satellite.

(A) *Semi-major Axis:* It is half of the length of the elliptical orbit of satellite. The atmospheric drag forces are more conspicuous near the perigee which is directly associated with the semi-major axis. The effect of atmospheric drag forces on the semi-major axis can be analysed through equation 13.

$$a = -\frac{C_d\ A a\rho}{m} n e^{\alpha\ cosE} \frac{(1+e\cos E)^{1/2}}{(1-e\cos E)^{3/2}} \tag{13}$$

(B) *Eccentricity:* It is the orbital element which describes the shape of the satellite orbit. Its value lies between zero and one. The atmospheric drag changes the orientation of the satellite by affecting its eccentricity which may lead the satellite to be unsynchronised with the ground station.

$$e = -\frac{C_d\ A a\rho}{m} n(1-e^2) e^{\alpha\ cosE} \frac{(1+e\cos E)^{1/2}}{(1-e\cos E)^{3/2}} \cos\ E \tag{14}$$

(C) *Mean Anomaly:* Mean Anomaly is calculated to find out the angle between the satellite orbital plane and the centre of the earth. The mean anomaly specifies the angular distance of satellite in the elliptical orbit which is calculated by the eccentricity and the eccentric anomaly.

$$M = \frac{C_d\ A a\rho}{m} n e^{-1} e^{\alpha\ cosE} \frac{(1+e\cos E)^{1/2}}{(1-e\cos E)^{3/2}} (1-e^3\cos E)\sin E \tag{15}$$

(D) *Argument of Perigee:* The atmospheric drag also affects the argument of perigee which is the angle between the Ascending node and Perigee. The intensity of effect can be well judged through equation 16.

$$\varpi = -\frac{C_d\ A a \rho}{m} n \frac{(1-e^2)^{1/2}}{e} e^{\alpha\ cosE} \frac{(1+e\cos E)^{1/2}}{(1-e\cos E)^{3/2}} \sin E \tag{16}$$

(E) *Inclination angle:* The effect of the atmospheric drag force is negligible on the inclination angle. It is the angle between the orbital plane and earth equatorial plane which does not contribute to the orbital perturbations as it falls on the z plane. It can be validated through eq. 17.

$$I = \frac{\cos(\omega+\theta) r F_z}{h} \tag{17}$$

RESULTS AND DISCUSSION

The analyses for five orbital parameters which are used to describe the orbit of the satellite are presented in this section. Figure 2 and 3 shows that the effect of gravitational and non-gravitational forces lead to attitude deviation of the satellite from its initial position (Barrio & Serrano, 2008).

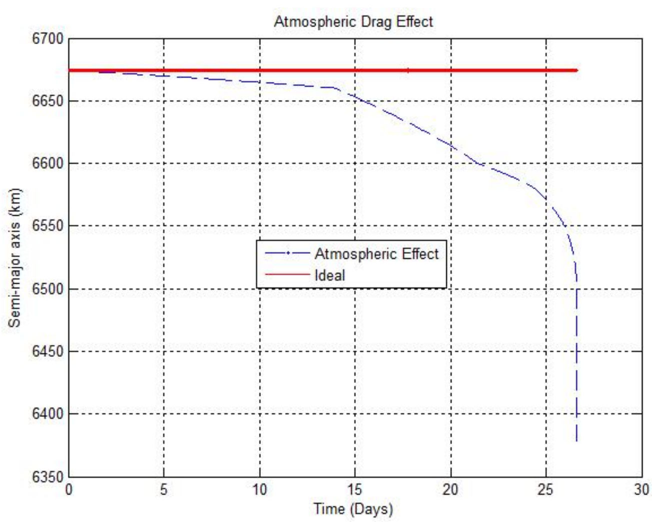

Figure 4. Effect of atmospheric drag on semi-major axis

The effect of atmospheric drag on semi-major axis is shown in Figure 4. It is observed that in ideal condition (under no drag conditions), the value of semi-major axis remains constant with respect to number of days but reduces as number of days increases under the circumstances of atmospheric drag. On the 20th day, the value of semi-major axis observed is 6614.7 but in ideal condition it is 6674.34, so it is observed that the drag effect compresses the orbit of satellite. The shape deviates and size of the orbit shrinks due to these perturbations.

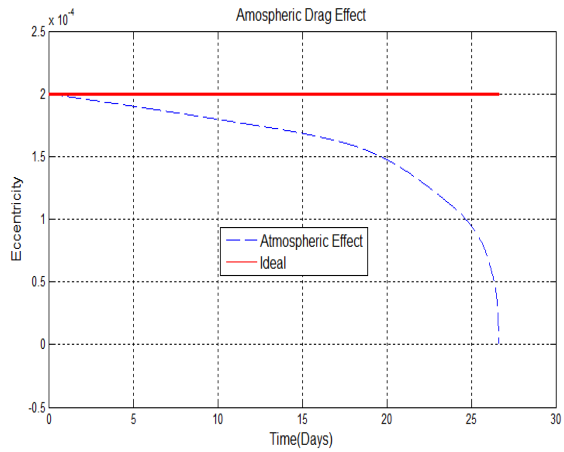

Figure 5. Effect of atmospheric drag on eccentricity

Figure 5 depicts the eccentricity of orbit under ideal and affected conditions. On 20th day from initial state, the value of eccentricity is 0.00014 which was 0.00020 in ideal condition. It is clearly that atmospheric drag not only compresses the semi-major axis but also changes the shape of the orbit which in turn may break the satellite link. The value of eccentricity is defined as 0 for a circular orbit, values between 0 and 1 form an elliptical orbit, 1 is a parabolic escape orbit, and greater than 1 is a hyperbola orbit.

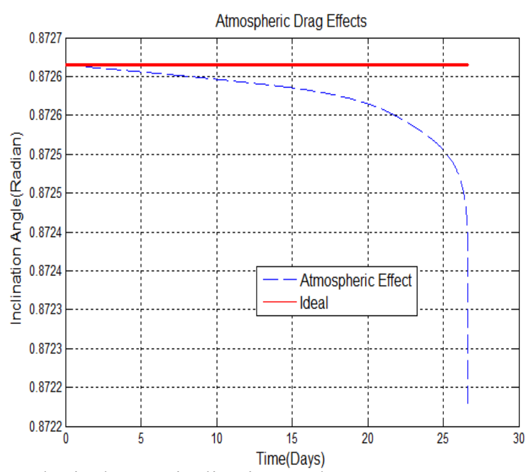

Figure 6. Effect of atmospheric drag on inclination angle

The effect of atmospheric drag on inclination angle is shown in Figure 6. The inclination angle is 0.8726 which remains the same in ideal condition but in adverse conditions it increases abruptly and then decreases as the day passes i.e. on 20th day, it is 0.8726 and on 25th day, it is 0.8725. After the 25th day, the value of inclination angle becomes constant.

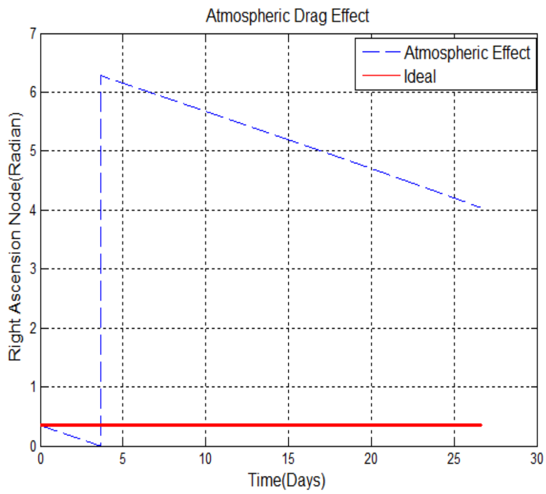

Figure 7. Effect of atmospheric drag on Right Ascension node

Figure 7 shows the effect of atmospheric drag on right ascension node. The ideal value is 0.35 for right ascension of ascending node. The value of RAAN due to drag initially reaches to 0.35 and then rapidly decreases to 0 on 4th day. Therefore, drag makes the right ascension node to deflect from its desired value.

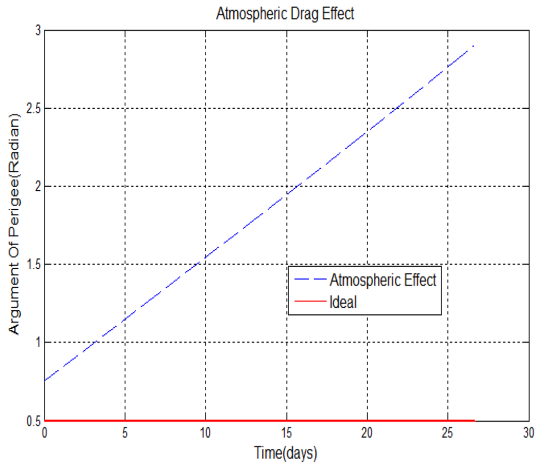

Figure 8. Effect of atmospheric drag on Argument of perigee

The effect on argument of perigee is seen in Figure 8; it increases linearly as the number of days passes. With assumption of atmospheric drag conditions, the argument of perigee initially is 0.7592 and reaches to 2.365 on 20th day.

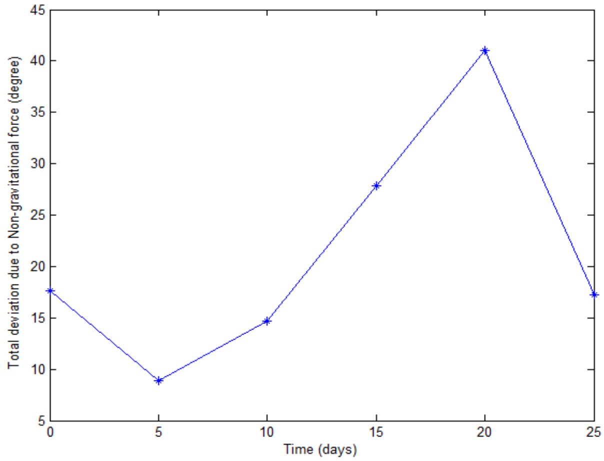

Figure 9. Variation of latitude and longitude due to Atmospheric drag

Figure 9 highlights the effect of non-gravitational force on the latitude and longitude of satellite orbit with respect to time. It is analysed that the influence of this effect is dominant after 10 days from the initial state.

Table 2
Variance in Orbital Parameter due to Atmospheric Effect

Day	Semi-major axis(a)(km)	Eccentricity(e)	Inclination Angle(i) (Radian)	Right Ascension of Ascending Node(Ω) (Radian)	Argument of Perigee(w) (Radian	Latitude, Longitude (Degree)
1st	6674.34	0.00020	0.8727	0.35	0.7592	44.8549,-157.5967
5th	6670.73	0.00190	0.8727	6.156	1.153	48.3106,-144.2983
10th	6665.2	0.00179	0.8726	5.682	1.546	49.9182,-129.5558
15th	6654.4	0.00168	0.8726	5.184	1.956	49.3820,-114.3120
20th	6614.7	0.00014	0.8726	4.699	2.365	46.7929,-100.0968
25th	6572.1	0.00009	0.8725	4.202	2.671	-30.9152, 85.9666

All the numerical values for the parameters mentioned in this section are given in Table 2 which shows orbital parameter values under ideal and adverse conditions. It also shows the influence of the atmospheric drag on the orbit of the satellite.

CONCLUSION

The prediction process requires the consideration of orbital parameters and the pre-determined period for exact prediction. Due to the atmospheric drag force, the inter satellite distance decay is also observed. In this paper, a novel method to calculate the deviation in orbital parameters is introduced to analyse the effect of atmospheric drag force; it is more effective on the semi-major axis and eccentricity which describes shape of the orbit. The changes in the orbital parameters directly affect the coordinates of the satellite which in turn may land up to loss of control over the satellite. Thus, the proposed method predicts the future coordinates of the satellite under the real-time conditions to prevent such problems.

REFERENCES

Al-Bermani, M. J. F. (2010). Calculation of Solar Radiation Pressure Effect and Sun, Moon Attraction at High Earth Satellite. *Journal of Kufa-Physics, 2*(1), 17-21.

Ali, Q., & Montenegro, S. (2014). A Matlab Implementation of Differential GPS for Low-cost GPS Receivers. *TransNav: International Journal on Marine Navigation and Safety of Sea Transportation, 8*(3), 343-350.

Barrio, R., & Serrano, S. (2008). Performance of perturbation methods on orbit prediction. *Mathematical and Computer Modelling, 48(*3), 594-600.

El-naggar, A. M. (2012). New method of GPS orbit determination from GCPS network for the purpose of DOP calculations. *Alexandria Engineering Journal, 51*(2), 129-136.

Hobbs, D., & Bohn, P. (2006). Precise orbit determination for low earth orbit satellites. *Annals of the Marie Curie Fellowships, 4*, 128-135.

Kandula, J., Kumar, G. S., & Bhasker, B. (2016). Experimental analysis on drag coefficient reduction techniques. *Proceeding of 4th International Symposium on Environment Friendly Energies and Applications*. Belgrade, Serbia: IEEE. Retrieved from http://ieeexplore.ieee.org/document/7748771/

Kuznetsov, V. B. (2016). Parabolic orbit determination. Comparison of the Olbers method and algebraic equations. *Solar System Research, 50*(3), 211-219.

Moe, K., & Moe, M. M. (2011). Operational models and drag-derived density trends in the thermosphere. *Space Weather, 9*(5), 1-6.

National Aeronautics and Space Administration (n.d.). O*rbital Elements*. Retrieved from https://spaceflight.nasa.gov/realdata/elements/

Pardal, P. C. P. M., Kuga, H. K., & de Moraes, R. V. (2009). A discussion related to orbit determination using nonlinear sigma point Kalman filter. *Mathematical Problems in Engineering, 2009*(2009), 1-12.

Santos, W. G. D., Rocco, E. M., & Carrara, V. (2014). Trajectory Control During an Aeroassisted Maneuver Between Coplanar Circular Orbits. *Journal of Aerospace Technology and Management, 6*(2), 159-168.

Yang, Y., Yue, X., & Dempster, A. G. (2016). GPS-based onboard real-time orbit determination for leo satellites using consider Kalman filter. *IEEE Transactions on Aerospace and Electronic Systems, 52*(2), 769-777.

Yi, P., Huafu, L., Zhuxian, Z., Feijiang, H., Chenglin, C., & Lu, F. (2016). An Algorithm for Inter-Satellite Autonomous Time Synchronization and Ranging in the Beidou Navigation Satellite System. *International Journal of Future Generation Communication and Networking, 9*(7), 229-238.

Yu, X., Yang, Y., & Ding, J. (2013). Satellite network design method applicable to orbit determination and communication for GNSS. *Proceedings of 4th International Conference on Software Engineering and Service Science.* Beijing, China: IEEE. Retrieved from http://ieeexplore.ieee.org/document/6615447/

Zaminpardaz, S., Teunissen, P. J., & Nadarajah, N. (2017). IRNSS/NavIC L5 Attitude Determination. *Sensors, 17*(2), 274-287.